# Final Project
# Using the Rate of Change of Cross-Sectional Area Slices of the Left Ventricle as a Means for Quantifying Sphericity in 3D Cardiac Ultrasound Images

BME 543L: Cardiac Ultrasound
Tong Fu, Jose Rivera, and Kathleen Embury

## Abstract

As the population of the United States continues to grow older, the prevalence of heart disease increases. Ventricular remodeling is a result of a number of heart conditions where the left ventricle "balloons" outward as a result of compensatory mechanisms the heart must undergo to be able to pump blood efficiently to the rest of the body. 3D ultrasound technology has brought about novel ways to analyze the degree of dilation in a person's left ventricle, but the volume of data that must be processed and the poorly defined ways of analyzing this data have resulted in a barrier towards using 3D ultrasound with greater frequency in the clinic. In this project we propose a novel way to determine the sphericity of the ventricle using 3D ultrasound data and a novel way to automate one of the previous methods that has been used to determine the sphericity of the ventricle using 2D ultrasound data. We believe that the use of these two methods combined will result in greater diagnostic power to render 3D ultrasound more useful towards saving the lives of patients in the clinic.

## Background

Echocardiography is the leading tool used for diagnostic and prognostic purposes related to diseases and disorders of the heart (1). Heart disease is the leading cause of death in the USA, and a major cause in the rest of the world (2). With the development of 3D cardiac ultrasound, and the resultant improvement in diagnostic and prognostic accuracy, these statistics can be drastically reduced. 3D Ultrasound presents numerous advantages over 2D as it allows for the real-time viewing of major valves and the four chambers of the heart. In this way, 3D echocardiography allows for an appreciation of depth within ultrasound images that 2D lacks. Valves can be fully seen, along with their relationship to surrounding structures, giving a more realistic representation of the heart. The physician is also able to view the heart from multiple different perspectives, including "en face" slices looking directly into a valve to achieve the "surgeon's view." The images are also simply easier to interpret since they are more realistic. 2D ultrasound relies on assumptions about the geometry of the chambers, as well as the number of available views, to approximate volume. However, with 3D, voxel count is used based on an automated or semi-automated border detection software, allowing for a far more accurate evaluation of chamber volumes without the need for geometric modeling. Finally, data can be taken over an entire cardiac cycle to analyse volume and flow changes over time (3, 4). As a result of these and numerous other advantages, 3D echocardiography has fast become increasingly popular over 2D.

These improvements in ultrasound with the development of 3D echocardiography have allowed for earlier detection of issues, as well as a better guided treatment plan (2). Using the higher accuracy of volume estimations, clearer anatomical views, and blood flow analysis over

time, a physician is better able to determine structural abnormalities or issues with leaking valves present not only for a better guided treatment plan, but also for earlier diagnosis of diseases. However, even with this simplified viewing, it is often still difficult to effectively evaluate a patient without years of experience detecting abnormalities. Even with this, changes that indicate abnormalities can be quite small and indetectable even to the most trained eye. A quantifiable measure that a physician can quickly see is therefore crucial for the advancement in streamlined and more accurate diagnosis and prognosis, as well as earlier detection.

Sphericity of the left ventricle has long been used as a way to quantify the change in the chambers of the heart as a result of heart diseases and disorders, or leading to these diseases (4). This determines how similar the LV is to a sphere geometrically, and can be calculated in one of two ways. For both methods, the long axis of the ventricle must be determined, and a "Sphericity Index" (SI) is determined. The long axis is obtained using an apical, or apical 4 chamber view so that the entire left ventricle is visible, and by taking the length from the inner wall tip of the apex back to the middle of the middle of the mitral valve (5). The dimensional SI also requires a short axis measurement, which is a line perpendicular to the long axis that spans the middle of the LV at its widest point, aligning the base and apex of the heart. The dimensional SI is simply the ratio of the short axis length to the long axis length, or vise versa. This process is displayed in Figure 1. Volumetric SI is found by calculating the volume of a hypothetical sphere that would have the long axis as its radius , and is the ratio of this volume to the actual volume of the LV as found using 3D volume analysis software(5, 6).

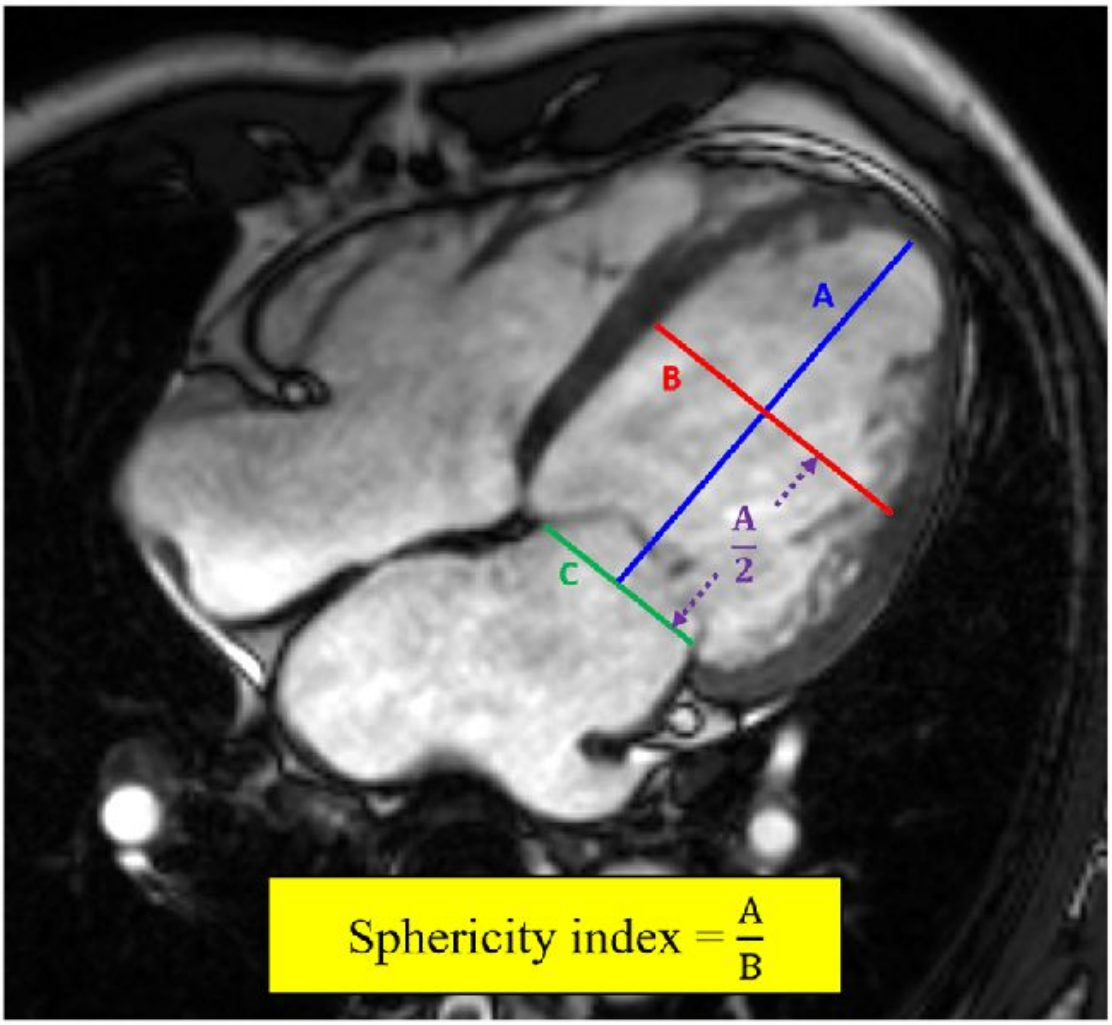


**Figure 1.** *Demonstration of the measurements needed to calculate SI . A is the long axis, while B is the short axis (6).*

It has been found that following a myocardial infarction, or heart attack, a phenomenon known as left ventricular remodeling occurs. LV remodeling is the process by which the cellular structure of the left ventricle undergoes geometric changes as a result of a heart disease or disorder (7). There are three patterns of LV remodeling: concentric, eccentric, and myocardial injuries. Concentric remodeling occurs as a result of pressure overloads from hypertension, or high blood pressure, causing thicker heart walls (8). Eccentric causes heart cells to lengthen, and occurs from volume changes from valvular regurgitation. Each of these causes scar tissue to build up within the heart (7,8) . As a result of a myocardial infarction, or a heart attack, blood flow is restricted or completely cut off to a certain area of the heart, generally the apex (9). This causes the cells at the apex to elongate, interspaced with fibrous scar tissue. The interstitial spaces between cells further up along the walls of the chamber will collect collagen, and the cells themselves undergo hypertrophy, meaning they increase in size. Starting with the thinning of the

cells at the apex, a spherical geometric change begins to occur. As time goes on and the walls thicken further up the heart, this spherical change becomes more pronounced (9,10). Therefore, the level of sphericity can be used to determine how healthy a person's heart is. Heart failure and eventually death can occur since remodeling changes the inflammatory and immune cell responses of the heart, if it is not caught soon enough and treatment starts (11). .Additionally, the fact that the heart has become more spherical and walls thickened in and of itself has detrimental effects on its function. First, the wall tension and stress has been redistributed along the ventricle. The heart is also less efficient at pumping blood as a result of the shape change and thicker, stiffer walls, which also causes mitral valve regurgitation. This results in a lower ejection fraction, and lower end systolic volume (12, 13).

Sphericity measures how ellipsoid the LV is, and therefore can be used to say if the LV has become more spherical, indicating remodeling. Therefore, earlier detection of remodeling is necessary in order to manage patients with this structural change and to more accurately determine their prognosis (10). Reverse remodeling can also occur, and has a higher rate of occurrence if the problem is caught earlier. This means that even if the left ventricle has started to become more spherical, with treatment, it can regain some of its original shape (14). The level of sphericity can also be used to determine the correct treatment, such as whether an ICD is necessary (15). With a quantifiable measure, a doctor is able to more accurately assess a patient.

Previous studies have looked into how specific sphericity numbers relate to cardiac diseases, as well as treatment plans. It has generally been found that those who have undergone myocardial injury or disease do develop a more spherical left ventricle in both diastole and systole, and that each of these can be used to determine a person's prognosis (16) . Several studies have found that sphericity of patients who underwent mitral valve replacement and died in the hospital was much higher than those who survived . The average ratio of short to long axis in these studies was approximately 0.6 (17, 18, 19). The 10 year survival rates of patients following a heart attack was also found to be much lower for those with an index from 0.6-0.8 (20). Other studies have been done to see if sphericity can predict the occurrence of diseases. Some have found that higher sphericity is correlated with a later development of coronary heart disease and heart failure (21). Other studies have been done to determine if sphericity measures could be used to prescribe specific treatments. Notably, it has been found that patients with an SI of 0.65 or higher benefit from an ICD (22).

However, much of this previous research has several limitations that have prevented any of these SI measures from being used clinically. It is generally found that healthy individuals with ellipsoid left ventricles have SI's all around 0.5, but the measures for SI that correlates to a worse prognosis or diagnosis vary quite a bit across these studies from 0.6--0.9 (16-22). There is no generally agreed upon method to process the images, or which SI between volume or dimensional is superior. Most of these studies also ignore regional reshaping, since sphericity index is by nature a measurement of global sphericity (23, 24, 25). When tissue is first starting to thin and elongate at the apex of the heart, geometric changes occur just in this area, making

the apical area more spherical while the rest of the chamber remains ellipsoidal. Therefore, the SI will not detect any change, even though it is occuring (25). Early detection of these changes could drastically improve a person's likelihood of a better recovery since less heart tissue has been compromised at this point. Also, the sphericity index of a person with a simply dilated ventricle will remain the same as the ratio is constant. This occurs in eccentric hypertrophy in particular (26, 27). Therefore, the sphericity index can not detect the abnormalities present within such patients. Several studies have also utilized the 2D echo rather than the 3D echo. As discussed previously, 3D echocardiography is vastly more accurate and improved than 2D at detecting edges, structures, and depth of the chambers. Sphericity indices were also taken only with respect to a single plane in most of the studies, which does not take into account the perpendicular plane of the ventricle which may not be the same geometrically. Finally, these studies have, for the most part, ignored the need for an automated software that a physician could use to receive a sphericity measurement.

It is important to note a couple key studies that have attempted to solve these issues that previous studies have ignored. One study endeavored to solve the issue of regional geometric changes by defining a new index they called the "conicity index." This was also done to try to solve the issue of a dilated ventricle giving the same ratio for sphericity index. They would take the apical axis length, defined at the diameter of a circle that fits just the apex of the heart. Then, the conicity index was the ratio of the apical index to the short axis length. The patients' hearts did not have fully developed global sphericity, but did have some apical changes due to recent disease development or injury. It was found that the SI remained the same between healthy and dilated, or regionally changed patients, the conicity index did increase (28). This is displayed in Figure 2. This study does not, however, solve any of the other problems listed above, and like SI, conicity index was not found to be adequately consistent for any specific numbers to indicate anything other than a higher number was worse (28).

Another study attempted to optimize the SI itself in an effort to increase its diagnostic and prognostic precision and accuracy, as well as to solve the issue with identifying regional sphericity. This study took 2D cardiac ultrasound data from fetuses, and took 24 transverse slices of the ventricles, including the mid-basal apical slice. Both ventricles were studied simply because the purpose of the study went beyond correlating sphericity to diseases, but also to look at structural abnormalities in fetuses' hearts as a whole. The results of this study, however, are still applicable for sphericity index in general. A specialized cardiac computer software traced the boundaries of the ventricles, and this boundary overlaid onto a graph so that 49 points could be identified along this boundary correlating to arbitrary x, y coordinates. The 24 transverse slices were obtained by connecting opposite points perpendicular to the long axis length. The SI was then computed for each of the transverse slices, not just the central one. This process is displayed in Figure 3. The sphericity indices were then plotted and analyzed for hearts that had abnormalities compared to normal hearts. They were also analyzed to find any specific regions of the heart that displayed dramatically different SI's as a group. This study did find correlations

between diseased hearts in specific regions as compared to normal hearts (29). However, it still does not take into account the other issues raised with SI.

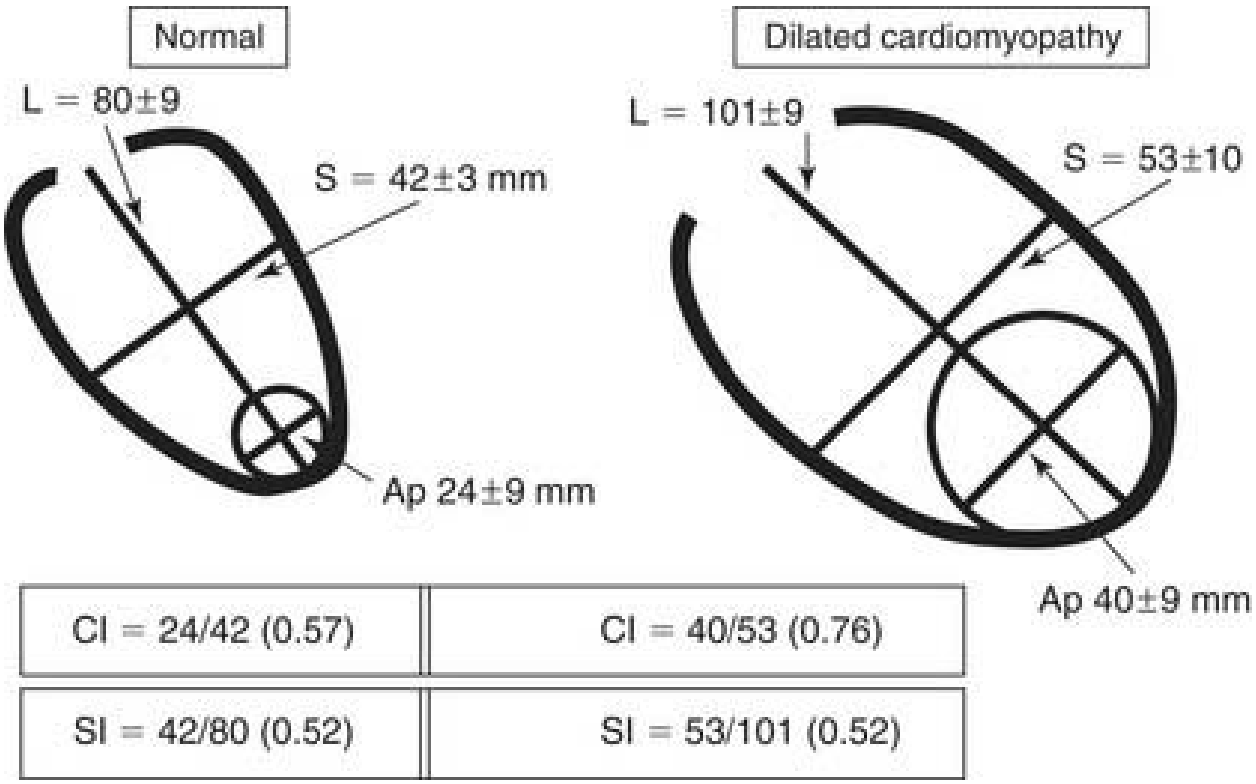


**Figure 2.** *Newly defined "conicity index" as compared to normal sphericity index (28).*

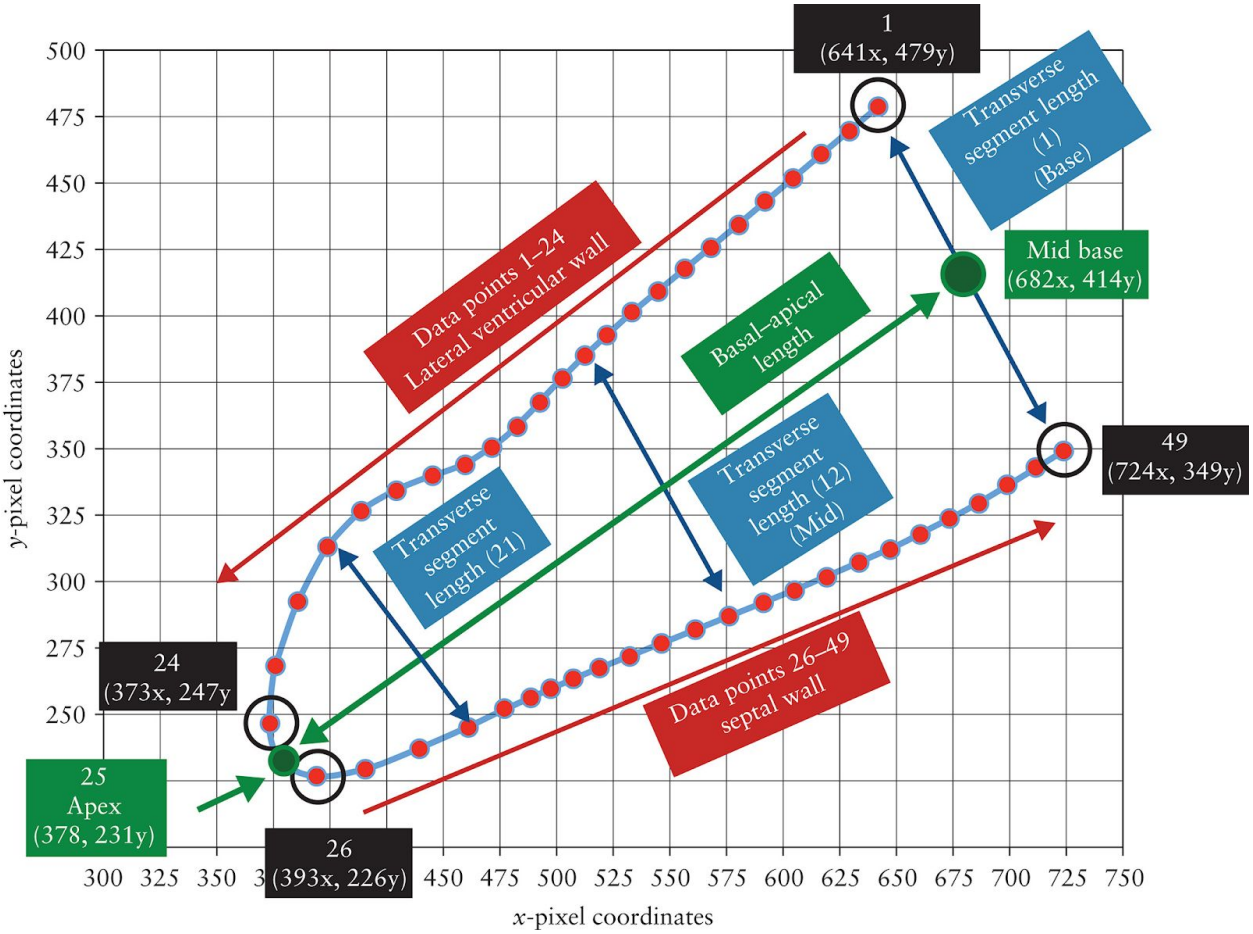


**Figure 3.** *24-Slice sphericity method (29).*

Because of all the limitations to research to date on sphericity, further work is necessary in order to optimize the process. This project aims to solve these issues by analyzing two methods of sphericity measurement. First, sphericity ratios will be found by taking mid-basal-apical lengths in two perpendicular planes of the left ventricle, the x and y direction, as will be described in the methods, using 3D cardiac ultrasound images. This will be done in an effort to more fully characterize how spherical the ventricle is by taking more planes into account using optimized 3D data. Next, the area rate of change of circular slices of the ventricle, taken from the apex of the heart up, will be found in order to account for regional differences in sphericity. An automated method for a physician to use so that she can receive a quantified number for the multiplane ratio method is also developed in order to allow for easy determination of the health of a patient which will hopefully better inform the physician of prognosis, diagnosis, or necessary treatment. All of this is done in an effort to produce a more accurate, reproducible method to calculate and convey sphericity of the left ventricle to optimize patient outlook.

## Methods

### *3D Echocardiogram Data Source*

3D cardiac ultrasound data was obtained from Dr. Cooper Moore's website through Duke for BME 265 - Ultrasonic Cardiac Imaging and Measurement. This is a former undergraduate course that has developed into the current BME 543L: Cardiac Ultrasound Imaging and Functioning. This website contains a database of seven .dcm files for seven different patient hearts. Data from the files for Patient 1 and Patient 2 were used in this project. In order to read the .dcm image data files for image analysis into a usable format, a Matlab script from this site was also obtained with Dr. Moore's permission (30). This code is included in Appendix A. Matlab R2018a was used for the subsequent image processing and analysis.

### *Image Processing*

In order to make the images more easily analyzed, image processing was performed. This was performed in an effort to make edges of the ventricle that would be used to place markers for lengths within the chamber could be more accurately marked, as well as provide a way for images to be filtered so that these measurements could be more consistent across images. The process by which individual slices were taken from the 3D data sets that corresponded to different time points will be explained in the "Sphericity Index Ratio" section of the Methods. These slices were processed by first resizing them, and turning them into a binary image using regional thresholds. Then, A Canny filter was applied to the resized images in an effort to detect edges. Finally, a code was developed to trace the boundaries of the ventricle using regional thresholds. The threshold filtered image was colored in for easy edge detection as well. This was done for all three planes used for measurements. These results are shown in Figure 4. The "jet" colormap was used, so there are varying colors in the last images. However, these are unimportant for the purposes of this project. They simply correspond to varying values of brightness for each pixel. In other words, after all the above filtering, each pixel is assigned a number value, with a lower number meaning a darker pixel. Each of these values is assigned a different color with the colormap. We simply used color to make the edges more defined, so the different colors are inapplicable. Full code is included in Appendix B. The most useful images for accurate edge detection were those produced by the boundary tracing and the simply binarized image following regional thresholding. The most accurate representation of the ventricle was chosen to be used to mark points for length measurements for each individual slice

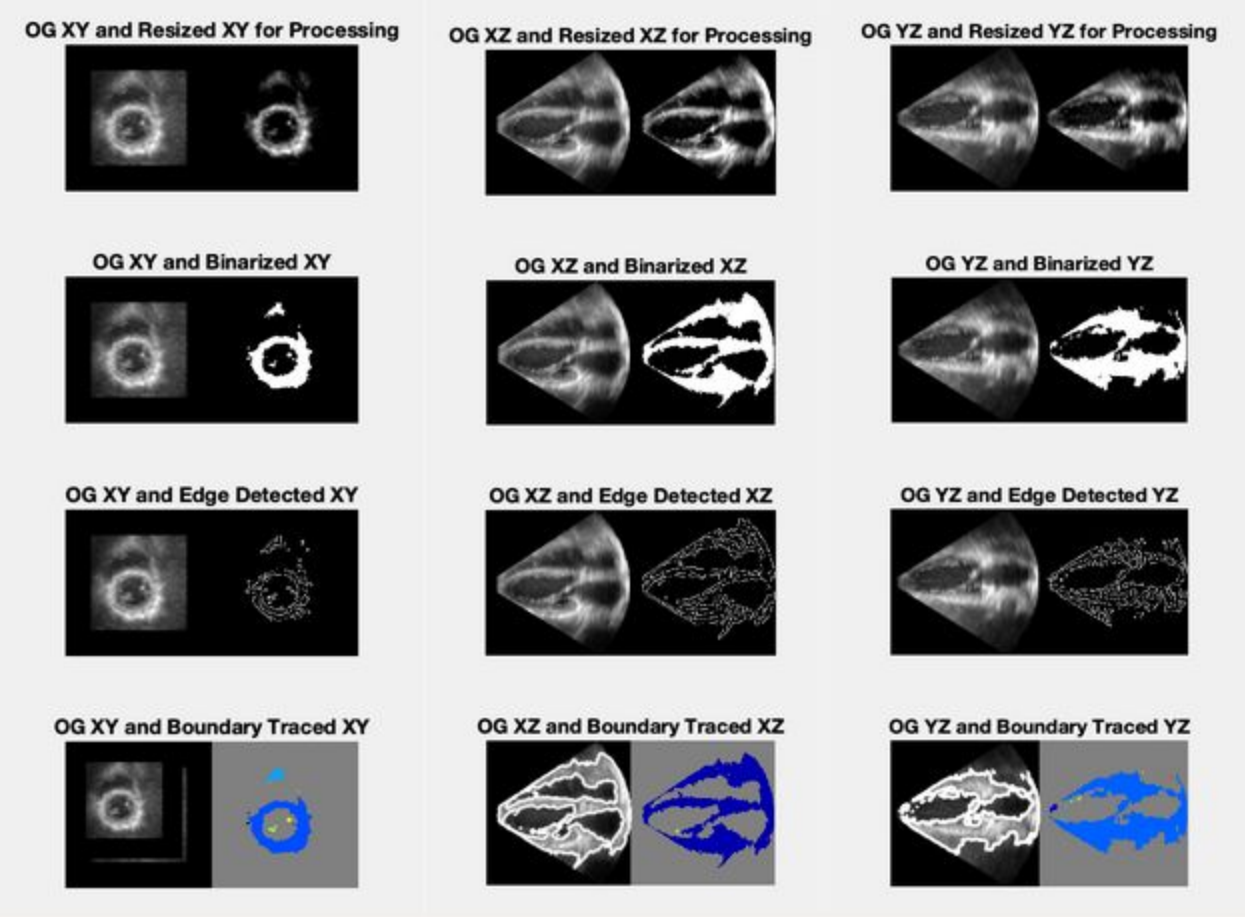


**Figure 4**. *Image processing outputs for each step of the filtering process.*

### *Sphericity Index Ratio*

The first method we used to calculate the left ventricular sphericity index (SI) was to reproduce the established technique that is examined by DeVore, Greggory, et al. (29). The SI in Devore's paper is evaluated and computed by finding the ratio of mid-basal-apical length to the transverse length of each of the 24 end-diastolic transverse segments. The method provides a broad way to determine the shape of the left ventricle, but it is conducted only with 2D ultrasound data.

The process was replicated in Matlab for all three planes (XY, XZ, and YZ plane). The XY plane is cut in the transverse view, the YZ plane is the sagittal view, and the XZ plane is the Coronal plaviewne. These correspond to the planes indicated in Figure 5.

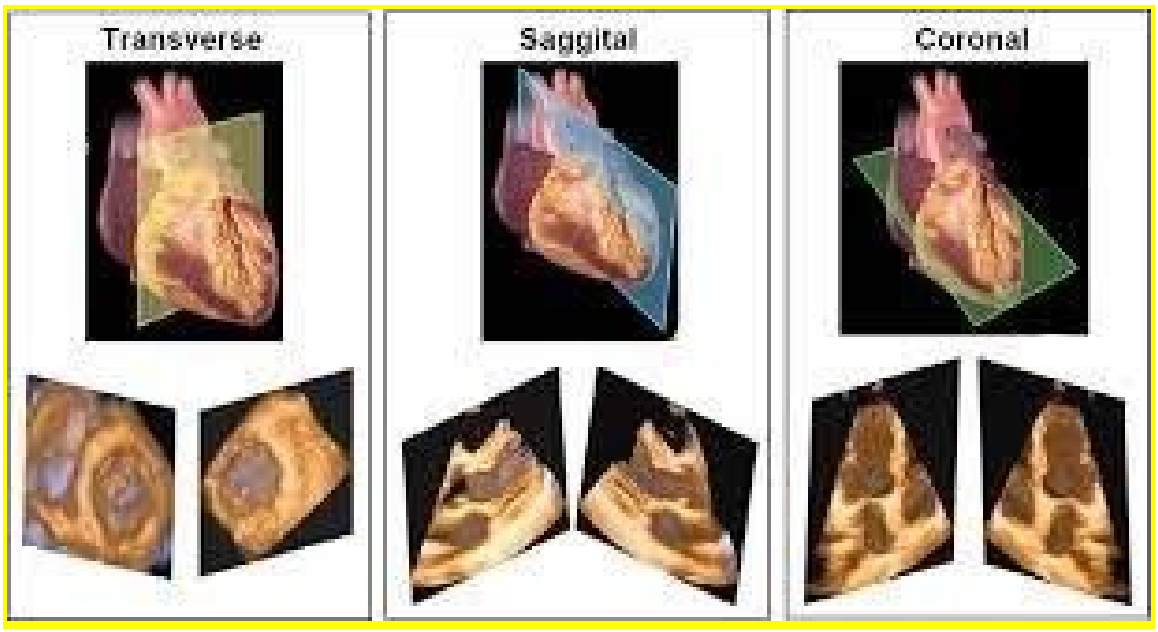


**Figure 5.** *Left: XY plane; Middle: YZ plane; Right: XZ plane*

For both patients, the middle slice of each plane was selected after the original heart echo data was resized to a cube. The middle slice in each plane was picked because it was the only slice that would overlap and intersect at the mid-point of the chamber with each other and together give an accurate representation of the heart. Since the echo data includes a time factor, an analysis between diastolic and systolic difference was considered. There are 11-time points for patient one and 25-time points for patient two. Of these, the best end-diastole and end-systole phase were selected by eye-balling and comparing the area of the ventricle and the mitral valve position. This process is illustrated in Figure 6.

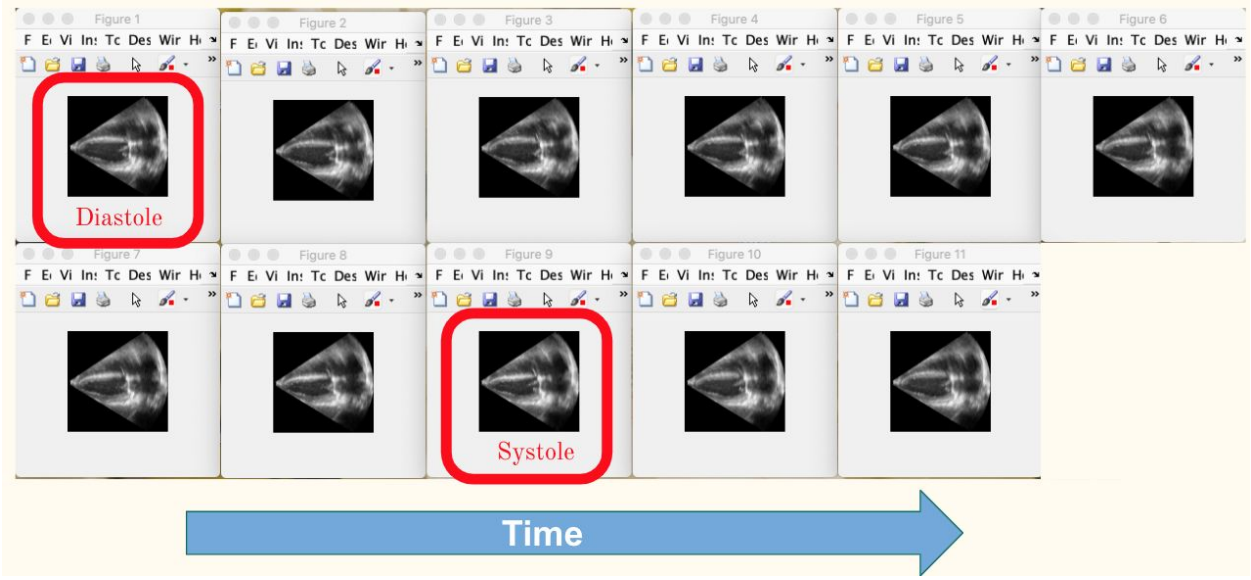

**Figure 6.** *An example (Patient 1, XZ plane, middle slice, time 1-11) of how systole and diastole phase was determined in matlab figures.*

The left ventricle was presumed to have roughly an ellipse shape. For each patient, four data points on the boundary of the ventricle were hand-picked from the Matlab figure of each phase and recorded: the top of the short axis, the bottom of the short axis, the left of the long axis, and the right of the long axis. This is shown in Figure 7. Short axis distance in pixels was then measured from a distance between the top and bottom point, and the long axis distance in pixels was the distance between the left and right points. The measurements in pixels were converted to units in centimeters by multiplying them by the pixel size, which was determined from dividing the width span (could also be depth span or height span depending on the direction in which the heart was being resized) by the number of pixels in the axis.

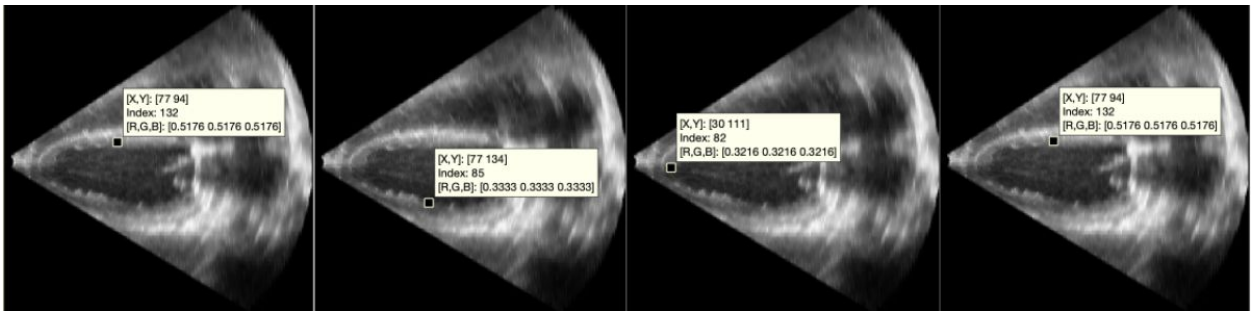


**Figure 7.** *Four pixels selected to find the long and short axis length*

The X-axis, Y-axis, and Z-axis each appeared twice in the three planes. For example, the Y-axis appeared in both the XY (long axis) and the YZ (short axis) plane. Therefore, the length of the left ventricle in each axis was averaged between the two planes before the final ratio calculation. A ratio of length in each dimension of the left ventricle, X: Y: Z, was computed. For convenience, X in the results was always scaled to be 1, and the sphericity ratio was thus 1/Z.

### *Area Rate of Change*

To explore the local effects of sphericity, a method looking at the rate of decreasing area within the heart will be utilized. This idea stems from the concept that the cross sectional areas of an ellipsoid change dramatically by looking at planes orthogonal to the long axis. On a sphere, however, the cross sectional areas of the sphere change significantly less rapidly due to the equidistant nature of the edge of the sphere to the center that ellipsoids do not possess. Therefore, by looking at the rates of change of the cross-sectional areas of the elliptical ventricle, an observation of a dilated ventricle can be determined for a patient's heart.

The area of an ellipsoid is determined using the equation $(\pi)(R_1)^2(R_2)^2$ where $R_1$ and $R_2$ are the short and long radii of the ellipsoid. As shown in Figure 8, the diameters of the ventricle

were extracted using the pixel extractor on MATLAB. The diameters were then divided by 2 and used to calculate the area of the ventricle, assuming its area is represented by the area of the ellipse generated by the two radii. These areas were generated for multiple cross sections in the ventricle 3 slices apart for a total of 16 cross sections. The areas of the ventricles were then plotted as a function of the position of the slices. Once this was plotted, the rate of the change of the cross sectional areas was calculated using the equation $|(A_2-A_1)/(S_2-S_1)|$ where $A_2$ is the cross sectional area of the following cross sectional area of $A_1$. $S_2$ is the plane number of $A_2$ and $S_1$ is the plane number of $A_1$. Because areas were chosen 3 slides apart, $(S_2-S_1) = 3$. The absolute value was taken to ensure that only the magnitudes of the change in area were compared. This plot simply gives a cardiologist a good relative idea of the shape of the ventricle by allowing for a view of the change in ventricle capacity across the position of the heart without any of the noise that comes with the image. This allows the physician to actually put a quantitative number to how much the ventricle is changing across position rather than simply using qualitative data from their eyes.

Because the heart is a dynamic object, measurements of the ventricles were taken at the extreme points of heart deformation at systole and diastole. This is important in analyzing the sphericity of the left ventricle, for it must be determined whether the sphericity calculation is independent of the heart cycle. Therefore, these methods were performed in the healthy heart of patient 2 and the diseased heart of patient 1 on the left ventricle for both diastole and systole to show that the change in cross sectional area in the heart of patient 1 was distinct enough from the change in cross sectional area for patient 2 to determine that patient 1's heart is dilated.

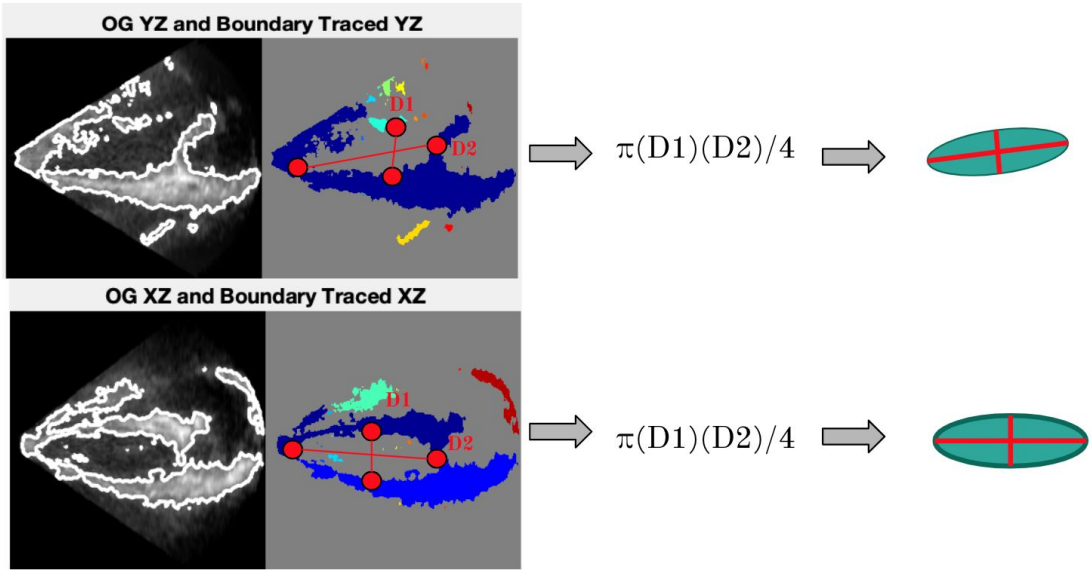


**Figure 8.** *Demonstration of the measurements to develop the elliptical area approximation of the ventricle.*

### *Automated Slicing*

A software was developed that takes in an .dcm file containing the 3D echo information, a set of data points selected by the user, and will automatically give the sphericity index of the heart. A message box will appear after the program starts, asking for inputs from the user. After the user feeds in the file name, at which time point they want to run the analysis, and for whatever times the user wants to repeat the measurements, the program will run. After the heart is resized, the middle slice in every plane will then be filtered (see the "Imaging Processing" section). A figure showing the middle slices in all three planes will show up, waiting for the user to select the points. The user will then hand pick six or more data points along the boundary of the left ventricle on each plane that they think would best represent the boundary of the ventricle. The process will repeat multiple times, depending on the number the user entered in the message box. Next, a function (30) is called to find the best fit to an ellipse for the given set of points. The ellipse fit-estimation method uses the Least Squares method with the estimator extracted from the conic equation of the ellipse. The more measurements it takes, the better the precision of the ellipse fit, but the more time the user will spend on selecting points. The program will then average the length of each of the dimensions and calculate the sphericity index using the method described in the above in the method section. An infobox will show up with both the X: Y: Z ratio and the sphericity index, giving the user an intuitive and straightforward perception of how round the heart is. Automation windows are displayed in Figure 9.

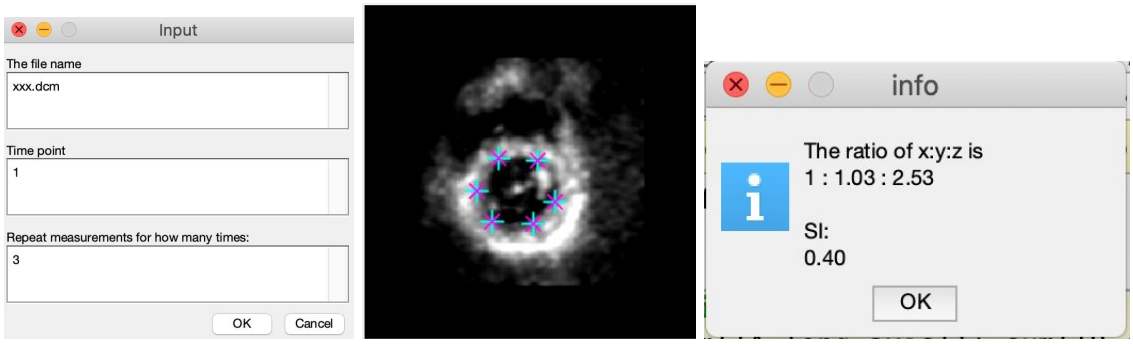


**Figure 9.** *Screenshots of the automated slicing software*

## Results

### *Sphericity Index Ratio*

For patient 1's left ventricle (dilated), the length ratio of the three dimensions (X: Y: Z) for the end-systole phase is 1:1.15:1.6 and 1:1.02:1.38 for the end-diastole phase. Since the established method of calculating the sphericity index is always done on the XZ plane (the plane with four chambers showing), we also computed the SI based on the XZ ratio. The heart in end-systole phase has a SI of 0.63, and in end-diastole phase has a SI of 0.72.

For patient 2's left ventricle (normal), the length ratio of the three dimensions (X: Y: Z) for the end-systole phase is 1:1.43:1.92 and 1:1.49:1.81 for the end-diastole phase. The heart in end-systole has a SI of 0.52, and at end-diastole has a SI of 0.55.

**Table 1.** *X:Y:Z ratio for patient 1 and patient 2 at systole and diastole*

| | Patient 1 (dilated) | Patient 2 (normal) |
|---|---|---|
| Systole | 1: 1.15: 1.64 | 1: 1.43: 1.92 |
| Diastole | 1: 1.02: 1.38 | 1: 1.49: 1.81 |

The sphericity index of the diastole phase for patient 1 is 15.9% larger (meaning the ventricle rounder) than that of the systole phase. The sphericity index of the diastole phase for patient 2 is 5.7% larger (meaning the ventricle rounder) than that of the systole phase.

The X: Y ratio barely changes in both patients compared to the X: Z ratio, confirming that the data was correct as the XY plane should have a circular (or nearly circle) shape. Patient 1's ventricle is longer in the Y-axis, and patient 2's ventricle is longer in X-axis. However, since this was only a single measurement taken at a one time point, this conclusion should not be drawn firmly.

Patient 2's heart is 23.6% more "elliptical" (SI smaller) in end-diastole (SI: 0.52) than that of patient 1 (SI: 0.61) in end-systole phase. It is also 14.8% more "elliptical" in end-diastole phase (SI: 0.55) than that of patient 1 (SI: 0.72) in end-diastole phase. A more detailed investigation into the data and what it indicates are discussed in the discussion section.

### *Area Rate of Change*

Figures 10, and 12 show the area of the YZ cross sections ( slices on the long axis of the heart into the left ventricle towards the right ventricle) as the viewer travels along the X axis. Measurements of these ventricles were taken every 3 slices due to the volume of slices that needed to be parsed. As shown in Figure 10, the ventricle area for patient 2 in diastole increases sharply, remains relatively constant at the annulus, and then decreases pretty sharply. Patient 1's heart is significantly more round due to the steady increase and decrease in area. Figure 11 shows how the area of each slice compares to the area after, thus giving a quantitative number to

the rate of change in the format of a bar graph. Because discrete points of area are being taken, this bar graph allows for a physician to easily pinpoint the location of a change in area and thus analyze how the area of the slice is changing between the slices of the area taken. This rate of change bar graph confirms the info displayed in Figure 10, that the rate at which the area in the ventricle increases and decreases in patient 2 is very fast while in patient 1, the rate of change is relatively sporadic and oscillating around 1.5 $cm^2/cm$.

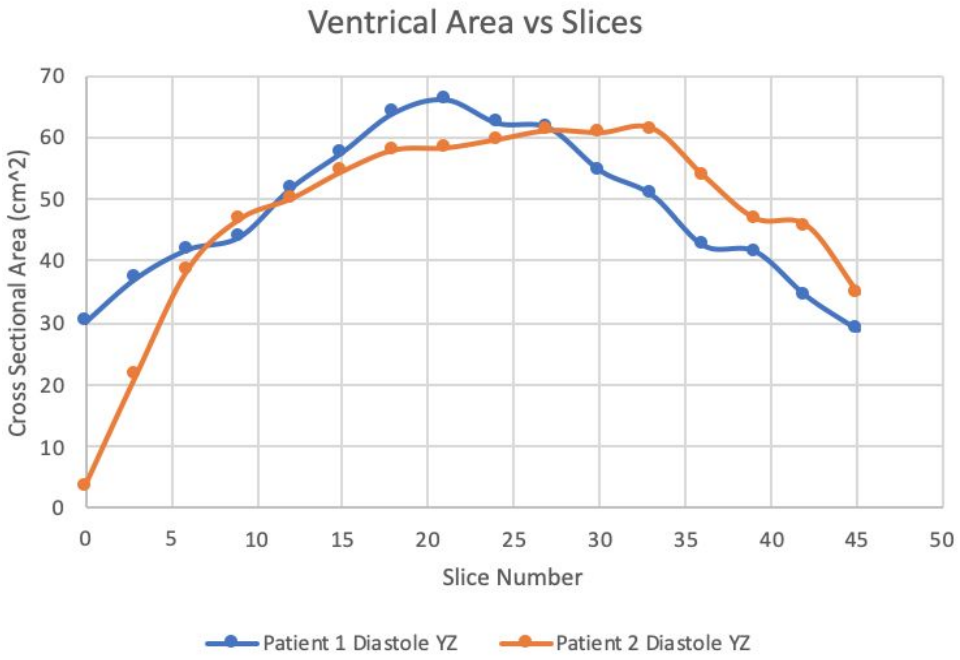


**Figure 10.** *The graph plots the cross-sectional areas of the generated ellipsoid. Cross sections move through the X axis and are in the YZ plane. This plot was generated while the heart was in diastole to determine whether there was a significant difference in ventricle area between patient 1 and 2.*

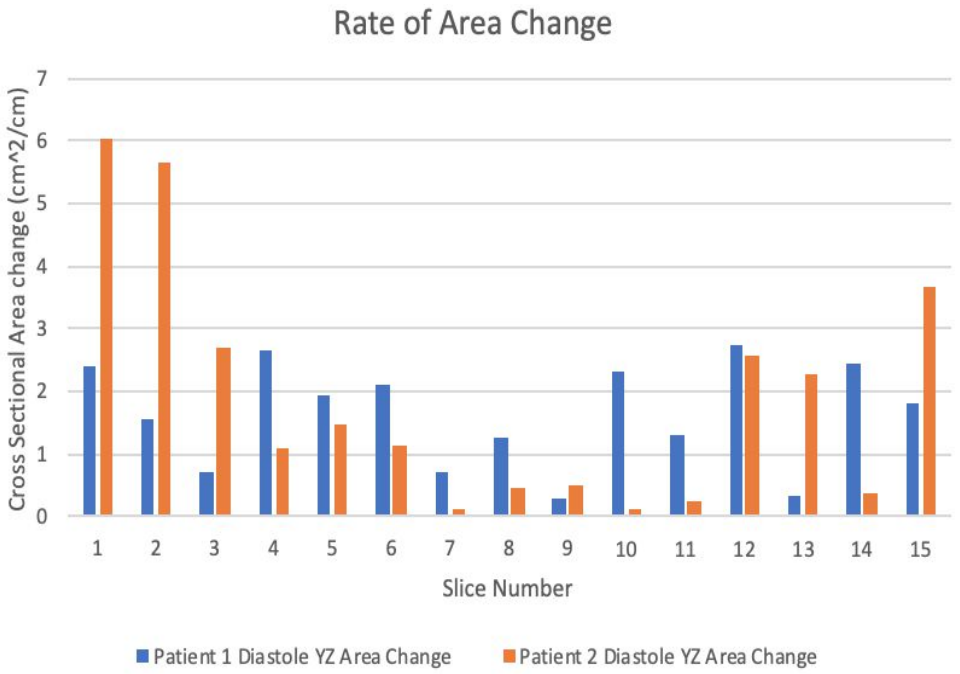


**Figure 11.** *The graph shows the rate of change between two cross-sectional areas of the generated ellipsoid. Cross sections move through the X axis and are in the YZ plane. This plot was generated while the heart was in diastole to determine whether there was a significant difference in the change in ventricle area between patient 1 and 2.*

Figure 12 shows the ventricle areas of patient 2 and patient 1 during systole. The curves look slightly more similar but one can see that the cross sectional areas of the left ventricle in patient 2 rise and plateau faster than the left ventricle in patient 2 . Nevertheless, the areas seem to meet together at roughly the same slice. Looking at the rate of change bar plot in Figure 13, patient 2's cross sectional area changes rapidly in the beginning, levels off, and then changes relatively rapidly at the end. Patient 1's rate of change data is significantly more sporadic but appears to be oscillating around a rate of change of about 2 cm^2/cm. This relatively constant rate of change can also be verified by looking at how the increase and decrease in area in Figure 12 appears to be very linear.

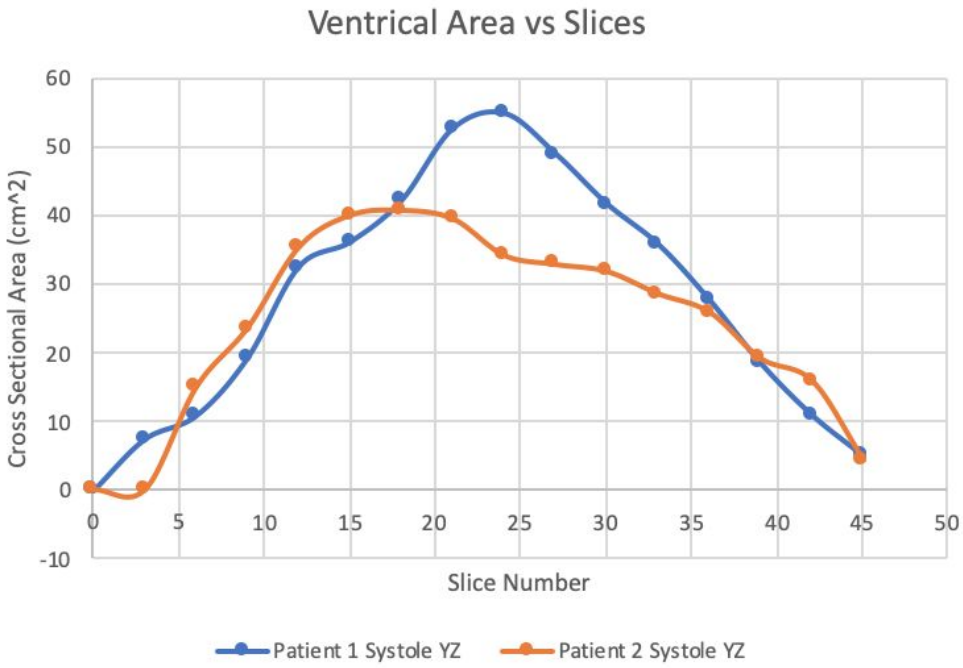


**Figure 12.** *The graph plots the cross-sectional areas of the generated ellipsoid. Cross sections move through the X axis and are in the YZ plane. This plot was generated while the heart was in systole to determine whether there was a significant difference in ventricle area between patient 1 and 2.*

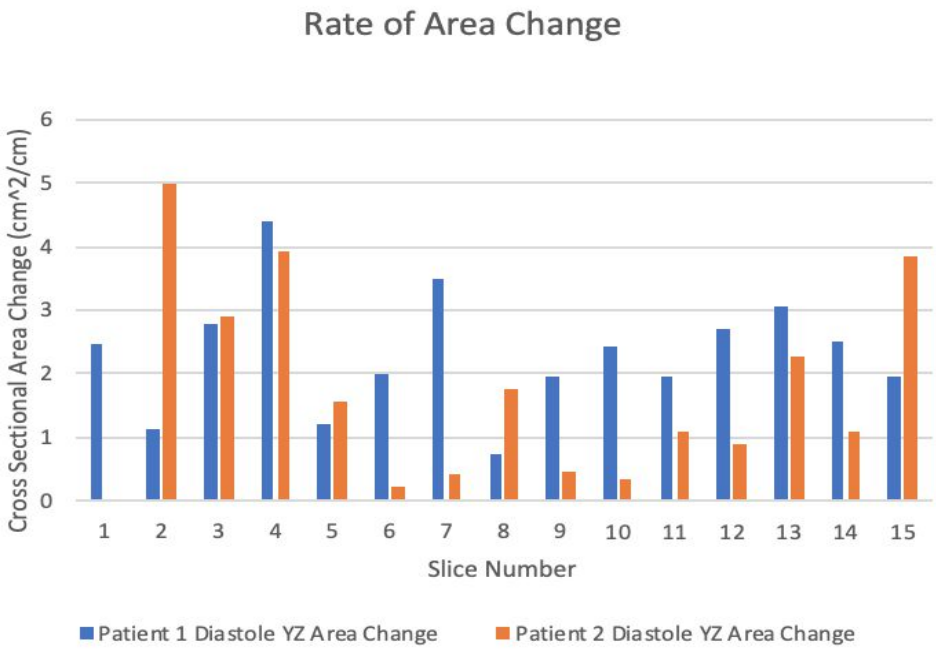


**Figure 13.** *The graph shows the rate of change between two cross-sectional areas of the generated ellipsoid. Cross sections move through the X axis and are in the YZ plane. This plot was generated while the heart was in systole to determine whether there was a significant difference in the change in ventricle area between patient 1 and 2.*

Figures 14 and 16 show the cross sectional area of the left ventricle across the XZ cross sections (four chamber view starting from the top of the heart and moving downward) as the viewer travels along the Y axis in diastole. Measurements of the ventricles were taken every 3 slices due to the volume of slices that needed to be parsed. As shown in Figure 14 the area of patient 1 appears to start large and does not appear to either increase or decrease very much until slice 21. Patient 2, on the other hand, increases and decreases its area much more rapidly. This can be quantified in Figure 15, where the rate of change of patient 2 is shown to be large in the beginning and ending slices but relatively constant in the middle. Patient 1 on the other hand appears to have much more sporadic rate of change, but the rate of change appears to oscillate around a rate of change of about 1.5 $cm^2/cm$.

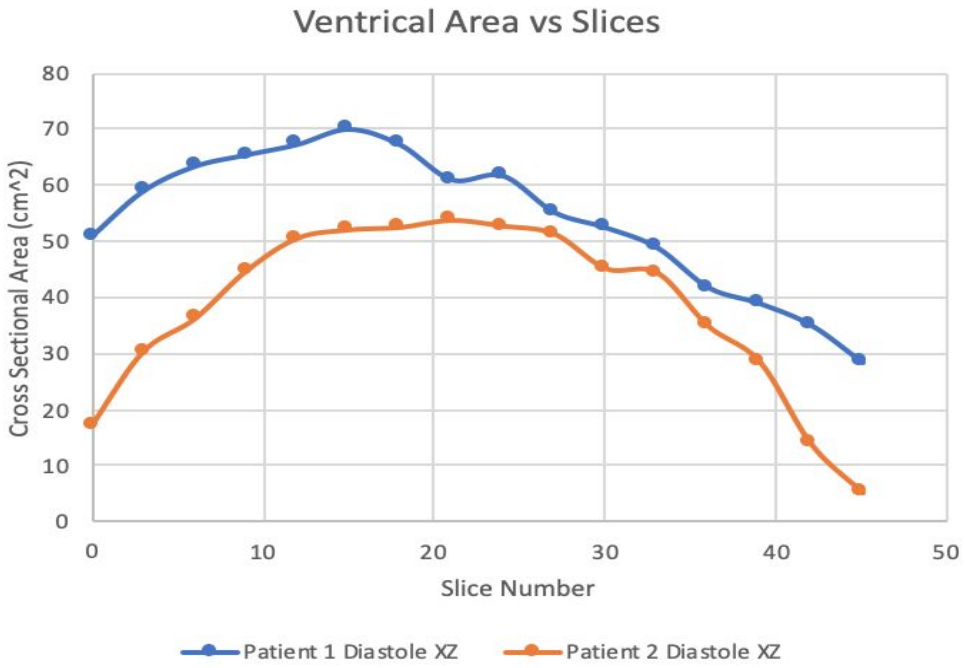


**Figure 14.** *The graph plots the cross-sectional areas of the generated ellipsoid. Cross sections move through the Y axis and are in the XZ plane. This plot was generated while the heart was in diastole to determine whether there was a significant difference in ventricle area between patient 1 and 2.*

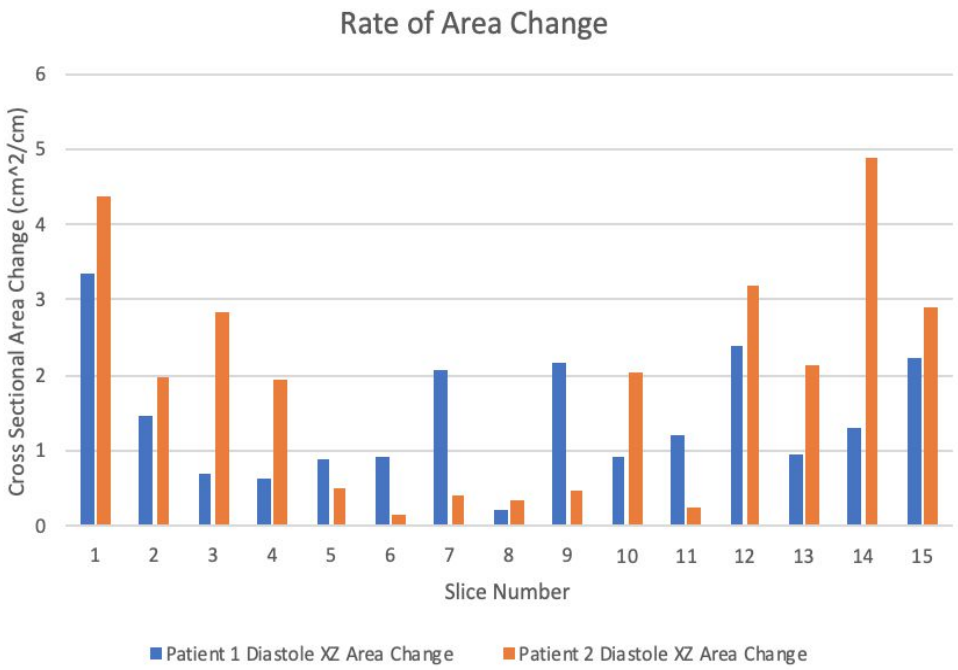


**Figure 15.** *The graph shows the rate of change between two cross-sectional areas of the generated ellipsoid. Cross sections move through the Y axis and are in the XZ plane. This plot was generated while the heart was in diastole to determine whether there was a significant difference in the change in ventricle area between patient 1 and 2.*

Figure 16 shows the ventricle areas of patient 2 and patient 1 during systole. The cross sectional areas of the left ventricle increase to the plateau in patient 1 faster than in patient 2. Overall though, the areas across the x axis make the ventricles look similar except for their overall size. Looking at the rate of change bar plot in Figure 17, patient 2's cross sectional area shows change rapidly in the beginning, levels off, and then changes rapidly at the end. Patient 1's rate of change data reflects fast uptake in area in the beginning along with a region of leveling off but exhibits a very constant rate of change as the area decreases.

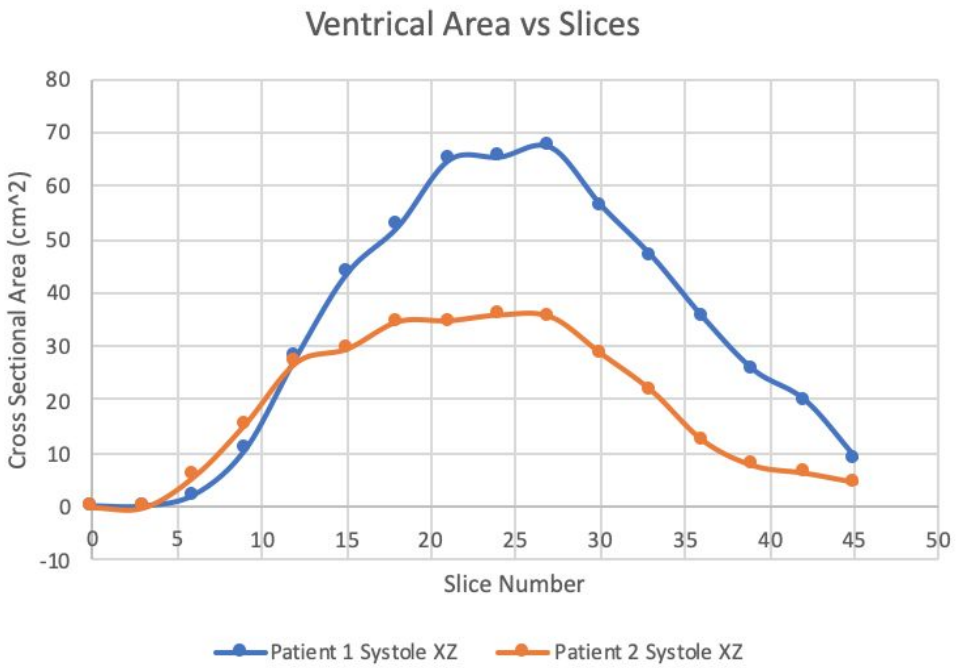


**Figure 16.** *The graph plots the cross-sectional areas of the generated ellipsoid. Cross sections move through the Y axis and are in the XZ plane. This plot was generated while the heart was in systole to determine whether there was a significant difference in ventricle area between patient 1 and 2.*

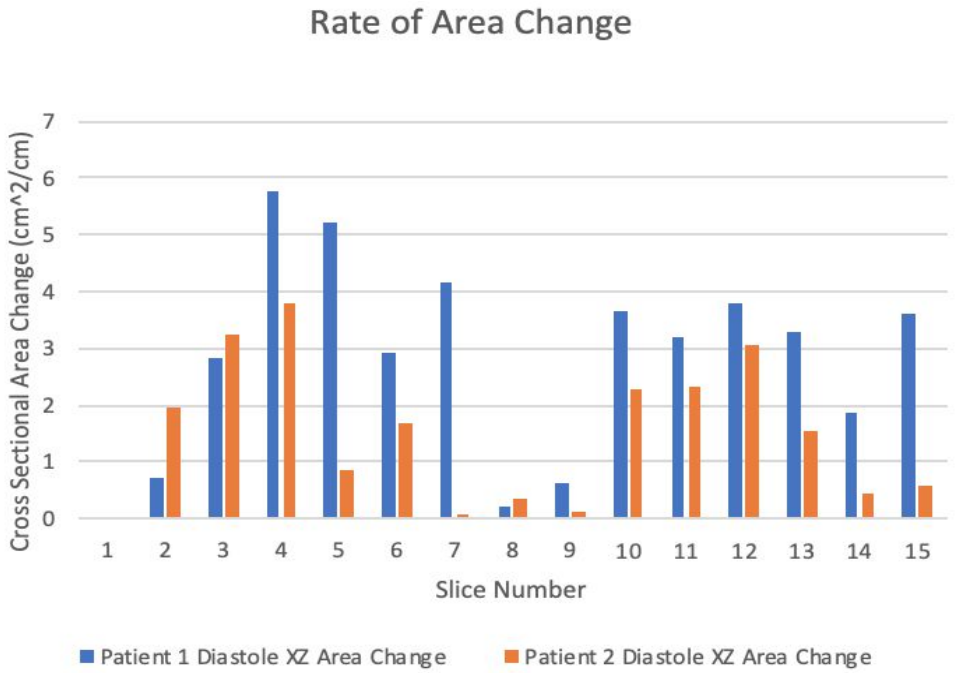


**Figure 17.** T*he graph shows the rate of change between two cross-sectional areas of the generated ellipsoid. Cross sections move through the Y axis and are in the XZ plane. This plot was generated while the heart was in systole to determine whether there was a significant difference in the change in ventricle area between patient 1 and 2.*

Overall it appears that Patient 1's left ventricle appeared to hold more volume due to the plots of patient 1 always possessing the slice with the largest cross sectional area.

### *Automated Slicing*

We tested the automated slicing software on both patient 1 (dilated) and patient 2 (normal) end-diastole ultrasound images. Patient 1 has an X: Y: Z ratio of 1:1.04:2.05 and a SI of 0.49. Patient 2 has an X: Y: Z ratio of 1:1.02:2.48 and a SI of 0.4. The X: Y ratio only changed by 1.9%, and patient 2 (normal) is 18.4% more "elliptical" than patient 1's (dilated) heart.

## Discussion

Results from the reproduction of the 24-segment sphericity index method indicate that for the two patients, the ventricle during diastole is "rounder" in shape compared to it is during systole. Diastole is the phase of the heartbeat when the heart muscle relaxes, and end-diastolic volume is the amount of blood that is in the ventricles before the heart starts to contract. As the heart contracts to pump blood out, the ventricle becomes more elliptical. This shape change from diastole to systole was observed to be more drastic in patient 1 (dilated heart, 15.7%) than inpatient 2 (normal, 5.7%). Moreover, the comparison between patient one and patient 2 suggests that patient 2's left ventricle was more "elliptical," and patient 1's left ventricle was "rounder," as seen in both systole phase and diastole phase.

SI correlates with the distance of papillary muscles, and a more significant distance between a papillary and higher degree of mitral regurgitation suggests that the shape is rounder. Mitral function is impaired when the sphericity index is high (31). The results we obtained were in agreement with the literature values. SI calculated by Di Donato, Marisa, et al., 230 was 0.52 for normal hearts diastole and 0.45 for systole. The number decreased significantly in patients with dilated cardiomyopathy with mitral regurgitation to 0.52 for diastole and 0.43 for systole. This also demonstrates that the dilated heart has a higher SI index, suggesting that the left ventricle is rounder and that in diastole it is rounder than it is in systole.

**Table 2.** *Comparison between literature SI values and our values*

| | Literature SI Values | | Our SI Values | |
|---|---|---|---|---|
| | Diastole | Systole | Diastole | Systole |
| Normal | 0.52 | 0.45 | 0.55 | 0.52 |

| | | | | |
|---|---|---|---|---|
| Dilated | 0.58 | 0.51 | 0.72 | 0.61 |

The established sphericity index method is easy and straightforward to implement and accurate if the heart is not tiled. However, the process is done manually, and the result is biased and determined by only four points picked along the boundary. Moreover, if the heart is tilted, one might need to use the distance formula to calculate the distance between two points.

The automated slicing method also shows that a normal heart has a smaller SI than a dilated heart, meaning that a normal heart is more elliptical. The XY plane didn't change significantly (2%). This method is efficient since the process is automated. It can also provide a quick, straightforward and intuitive number for doctors and physicians. The higher the SI, the more possible for the heart to be abnormal and dilated.

***Area rate of change***

The characteristic of a spherical heart would be a slower rate of cross sectional area change. This is because an ellipse shows greater change in these planes than a sphere since the shape of the ellipsoid is not bound to be equidistant from its center. A constant rate of cross sectional area change also signals a much more spherical shape since in a perfect sphere all of the cross sectional sections will be increasing or decreasing at the same rate assuming all of the cross sections are uniformly taken. To first analyze the sphericity of ventricles, the plane of the cross section that is to be looked at must be determined. The YZ plane will be analyzed first. In Figure 10, patient 1 shows a more spherical heart than patient 2 because the change in area is much more constant. This can be especially seen in the bar plot in Figure 11 of both patient's ventricles where the rate of cross sectional area in patient 1 appears to oscillate around 1.5 $cm^2/cm$ while patient 2's heart shows a strong rate of change. These measurements were performed in diastole when the heart was filled with blood when the heart would have the greatest capacity to be spherical due to the filling of blood in the left ventricle. In systole, when the heart is not filled with blood, the results appear to be less clear. This is because the dilated heart will appear more elliptical due to absence of blood to expand the ventricle to its spherical shape. This effect can be seen in Figure 12 in the faster uptake in cross sectional area in patient 1's left ventricle. Nevertheless, the area appears to increase pretty linearly in this plot. Patient 2's data, however, increases faster to its maximal cross section significantly faster despite decaying relatively linearly. Figure 13 shows how the rate of change of the areas for the cross sections in the two patients is significantly different. Specifically how the oscillation of patient 1's rate of change around 2 $cm^2/cm$ looks vastly different from how the patient 2's rate of change is large in the beginning and the end of the ventricle. Therefore, patient 1's heart can be differentiated being

spherical, but the diagnosis is harder to make due to presence of blood not exaggerating the "ballooning" nature of the left ventricle in patient 1.

In the XZ plane in diastole, the heart of patient 1 can be seen to be more dilated than patient 2. The cross sectional areas of patient 1 are overall larger than the cross sectional areas of patient 2. Again, the rate of growth of the areas in patient 2 is also faster than the much more constant growth of area in patient 1. In Fig 14, patient 2 shows the significant changing rates in area in the beginning and ending slices of the ventricle with a relatively constant area in the center. In Figure 15, it can be seen that Patient 1's rate of change is much more sporadic and again appears to oscillate around 1.5 $cm^2/cm$. Because of the more uniform rate of change values in patient 1's left ventricle and the relatively little change in cross sectional area, this left ventricle can easily be determined to be dilated in diastole. In systole, the dilation of ventricles are much more difficult to discern. As shown in Figure 16, the cross sectional areas of patient 1 are all higher than the cross sectional areas of patient 2. Nevertheless, the rate of change in ventricle area appears to be dramatic in the left ventricles of both patients. Nevertheless, Figure 17 shows that the area increase in patient 1 is very high especially compared to patient 2, despite patient 2 still possessing large changes in area. Furthermore, the area change in patient 1 after the plateau is very linear, showing signs of dilation in the ventricle, but it is difficult to tell.

Overall, it appears that measurement of the slices does depend on the time point that the heart is imaged. Specifically, the closer the heart is imaged to systole, the less the heart loses its dilated appearance, giving the ventricle a much more elliptical appearance. This is because when the heart is filled with blood, the ventricle takes on its full dilated shape to compare to a filled - non dilated left ventricle. In terms of slice dependence, it appears that both the YZ and the XZ plane can both be used to provide this information. In fact, both planes can be used to ensure that the heart is truly dilated by looking at different views. The short axis, or XY axis, view of the heart is missing. This is because the data was considered superfluous since the short axis would need to be spherical to embody a healthy ventricle, and while this would be helpful, the overall rate of area change would be very small until the heart begins to decrease to the apex. Therefore, looking at the XZ and YZ plane is simply more efficient to analyze if a person's ventricle is dilated.

This method can be more helpful than existing methods of measuring sphericity because local regions of dilation can directly be analyzed and caught with this method. Using methods from literature, the sphericity can only be measured from the center of the ventricle, thus the full 3D capabilities of 3D ultrasound are not being used. This method also simplifies the ultrasound for a physician to be able to focus solely on the numbers of the areas of the left ventricle. By isolating the spatial information of the left ventricle in a bar graph and a scatter plot, the data of the image is placed in a medium that is easier for the doctor to interpret and for a patient to understand. Other existing methods still require the comparison of the ratios of the diameters in the ellipsoid, and in 3D, this can be difficult to interpret and explain to a patient. Next, the doctor can physically see the morphology of the ventricle in how the area of the ventricle must sharply

increase and decrease, and can put physical numbers to the normal range of how the cross sectional area in the ventricle should be changing. Lastly, the automation of precious methods sparks an innovation in the precision and the speed of measurements being taken and will soon be applied to the method of changing areas.

The main drawback of the changing area method is the amount of radius measurements that must be taken. 16 different slices were taken for each ventricle for each heart cycle. The more slices, the more accurate the method, however, the method will take significantly longer since the radius measurements can only be done manually thus far. Therefore, one of the next steps is to try to automate the collection of the radii of the cross sections in the left ventricle. Another limitation is that since the calculation is dependent on the rate of change of the area in the ventricle, the radii calculations must be very precise. If the radii calculations are too off from the next radii calculation, the result will be a larger change in the cross sectional area of the ventricle, giving the doctor the impression that the heart is indeed elliptical when the error of the calculation is simply propagating into the rate of change of the ventricle. Therefore, automation must be very precise to ensure this method works. Lasty, this method only compared a healthy patient and a dilated patient. Ideally, there should be a larger sample size to ensure that the trends shown in this report apply generally.

## Conclusion

In this study, a novel method for the evaluation of sphericity of the left ventricle was explored in an effort to improve the reproducibility and accuracy of such measurements. Both a three-plane perspective on heart sphericity, and a rate of change analysis for regional variance was studied. An automated software for easy delivery of measurements to the user--most likely a physician--was also developed. It was found that the methods studied do indeed allow for relatively simple sphericity calculation and edge detection, returning values that are comparable to those in literature. However, due to the restraints on this project presented by the limited scope of the semester and the Covid-19 pandemic, there are several areas in which this work could be further explored. First and foremost, our study was limited most by a small data set with just two patient hearts. Therefore, with more data, this method could be verified. Also, specific measurements within our area rate of change method could be correlated with specific diseases. This could be done with the use of clinical trials. The automation could also be improved so that the code runs faster, and there is less chance of error due to the need for user input. Also, an automated system for the area rate of change measurements could be developed. Increasing the number of slices used would also allow for more accurate measurements. Curve fitting could be used in the final analysis as well for the area across position rather than just a discrete slope calculation. Finally, the image processing could be dramatically improved with

better filtering. Ultrasound images are inherently noisy, and difficult to generally filter as each image may require a different threshold.

This is a vitally important field for advancement as heart disease continues to be one of the biggest killers in the world. Though this project presents many areas of improvement, the overall methods developed hold promise as potential tools that could be used to significantly improve a physician's diagnostic, prognostic, and treatment-determination abilities given a 3D echocardiogram.

## References


1. National Heart, Lung, and Blood Institute, National Institutes of Health. What is echocardiography? 2011. [October 25, 2012]. Available at: http://www.nhlbi.nih.gov/health/health-topics/topics/echo/
2. Fryar CD, Chen T-C, Li X. Prevalence of uncontrolled risk factors for cardiovascular disease: United States, 1999–2010 pdf icon[PDF-494K]. NCHS data brief, no. 103. Hyattsville, MD: National Center for Health Statistics; 2012. Accessed May 9, 2019.
3. Lang RM, Badano LP, Tsang W et al. EAE/ASE recommendations for image acquisition and display using three-dimensional echocardiography. Eur Heart J Cardiovasc Imaging 2012;13:1-46
4. Badano LP, Boccalini F, Muraru D, Dal Bianco L, Peluso D, Bellu R, et al. Current clinical applications of transthoracic three-dimensional echocardiography. J Cardiovasc Ultrasound 2012;20:1-22
5. Udelson JE, Konstam MA. Ventricular remodeling fundamental to the progression (and regression) of heart failure. J Am Coll Cardiol 2011;5713:1477–9.
6. Monaghan M. J. (2006). Role of real time 3D echocardiography in evaluating the left ventricle. *Heart (British Cardiac Society)*, *92*(1), 131–136. https://doi.org/10.1136/hrt.2004.058388
7. Kaolawanich, Y. & Boonyasirinant, T. (2019). Usefulness of apical area index to predict left ventricular thrombus in patients with systolic dysfunction: A novel index from cardiac magnetic resonance. BMC Cardiovascular Disorders. 19. 10.1186/s12872-018-0988-9.
8. Opie LH, Commerford PJ, Gersh BJ, et al. Controversies in ventricular remodelling. Lancet (London, England) 2006;367:356–67.
9. Choi HF, Rademakers FE, Claus P. Left-ventricular shape determines intramyocardial mechanical heterogeneity. American journal of physiology. Heart Circ Physiol 2011;301:H2351–2361.
10. Pfeffer MA, Braunwald E. Ventricular remodeling after myocardial infarction: experimental observations and clinical implications. *Circulation.*1990; *81*:1161–1172
11. Konstam MA, Kramer DG, Patel AR, Maron MS, Udelson JE. Left ventricular remodeling in heart failure: current concepts in clinical significance and assessment. JACC Cardiovasc Imaging. 2011 Jan;4(1):98-108. doi: 10.1016/j.jcmg.2010.10.008. Review. PubMed PMID: 21232712.
12. Frieler RA, Mortensen RM. Immune cell and other noncardiomyocyte regulation of cardiac hypertrophy and remodeling. Circulation 2015;131:1019–30.
13. Zeng, Decai MD; Chen, Hui MD; Jiang, Chun Lan MD; Wu, Ji MD, PhD* Usefulness of three-dimensional spherical index to assess different types of left ventricular remodeling, Medicine: September 2017 - Volume 96 - Issue 36 - p e7968 doi: 10.1097/MD.0000000000007968
14. Reis Filho, J. R., Cardoso, J. N., Cardoso, C. M., & Pereira-Barretto, A. C. (2015). Reverse Cardiac Remodeling: A Marker of Better Prognosis in Heart Failure. *Arquivos brasileiros de cardiologia*, *104*(6), 502–506. https://doi.org/10.5935/abc.20150025
15. Anvari S, Akbarzadeh MA, Bayat F, Namazi MH, Safi M. Left ventricular sphericity index analysis for the prediction of appropriate implantable cardioverter-defibrillator therapy. Pacing

Clin Electrophysiol. 2018 Sep;41(9):1192-1196. doi: 10.1111/pace.13420. Epub 2018 Jul 11. PubMed PMID: 29931684.
16. Mannaerts HF, van der Heide JA, Kamp O, et al. Early identification of left ventricular remodelling after myocardial infarction, assessed by transthoracic 3D echocardiography. Eur Heart J 2004;25:680–7.
17. Vokonas PS, Gorlin R, Cohn PF, Herman MV, Sonnenblick EH: Dynamic geometry of the left ventricle in mitral regurgitation. Circulation 1973;48:786-795 9.
18. Gould KL, Lipscomb K, Hamilton GW, Kennedy JW. Relation of left ventricular shape, function and wall stress in man. Am J Curdiol 1974;34:627434 10.
19. Lamas GA, Mitchell G, Flaker GC, Smith SC, Gersh BJ, Basta L. MoyC L, Braunwald E, Pfeffer MS: The clinical significance of mi- tral regurgitation following acute myocardial infarction. Circula- tion I997;96:827-833
20. Douglas PS, Morrow R, loli A, Reichek N: Left ventricular shape, afterload and survival in idiopathic dilated cardiomyopathy. J Am CoNCurdiol1989;13:311-31a.
21. Ambale-Venkatesh B, Yoneyama K, Sharma RK, et al
Left ventricular shape predicts different types of cardiovascular events in the general population. Heart 2017;103:499-507.
22. Levine YC, Matos J, Rosenberg MA, et al. Left ventricular sphericity independently predicts appropriate implantable cardioverter-defibrillator therapy. Heart Rhythm 2016;13:490–7.
23. Fantini F, Barletta GA, Baroni M, Fantini A, Maioli M, Sabatier M, Rossi P, Dor V, Di Donato M. Quantitative evaluation of left ventricular shape in anterior aneurysm. Cathet Cardiovasc Diagn. 1993 Apr;28(4):295-300. doi: 10.1002/ccd.1810280406. PubMed PMID: 8462078.
24. Dor V, Montiglio F, Sabatier M, Coste P, Barletta G, Di Donato M, Toso A, Baroni M, Fantini F. Left ventricular shape changes induced by aneurysmectomy with endoventricular circular patch plasty reconstruction. Eur Heart J. 1994 Aug;15(8):1063-9. doi: 10.1093/oxfordjournals.eurheartj.a060629. PubMed PMID: 7988597.
25. Baur LH, Schipperheyn JJ, van der Wall EE, Reiber JH, van Dijk AD, Brobbel C, Kerkkamp JJ, Voogd PJ, Bruschke AV. Regional myocardial shape alterations in patients with anterior myocardial infarction. Int J Card Imaging. 1996 Jun;12(2):89-96. doi: 10.1007/bf01880739. PubMed PMID: 8864787.
26. Vieira ML, Oliveira WA, Cordovil A, et al. 3D Echo pilot study of geometric left ventricular changes after acute myocardial infarction. Arq Bras Cardiol 2013;101:43–51.
27. Yang H, Zeng Z. The value of three-dimensional spherical index in assessing different type of left ventricular remodeling. J Am Coll Cardiol 2015;66:C256–1256.
28. Di Donato M, Dabic P, Castelvecchio S, et al. Left ventricular geometry in normal and post-anterior myocardial infarction patients: sphericity index and 'new' conicity index comparisons. Eur J Cardiothorac Surg 2006;29(suppl 1):S225–30
29. DeVore, G.R., Klas, B., Satou, G. and Sklansky, M. (2018), 24-segment sphericity index: a new technique to evaluate fetal cardiac diastolic shape. Ultrasound Obstet Gynecol, 51: 650-658. doi:10.1002/uog.17505
30. Moore, C. (2012). BME 265: Ultrasonic Cardiac Imaging and Measurement. Retrieved from http://people.duke.edu/~jcm21/bme265/.

31. Tal Hendel (2020). Ellipse Fit (https://www.mathworks.com/matlabcentral/fileexchange/22423-ellipse-fit), MATLAB Central File Exchange. Retrieved April 30, 2020.

# Appendix A

**Matlab script for reading .dcm 3D echocardiogram patient heart data into usable format: readDicom3D.m (30)**

```
function [x,data] = ReadDicom3D(filename,MaxVolumes)

%function x = ReadDicom3D(filename,MaxVolumes)
%
% Inputs:
%   filename:   XYZ Dicom File Name (string) Exported from Sonos 7500 D.0
%   MaxVolumes: Limits the # of volumes to be read
%                   Default: 0 (read all volumes)
%
% Outputs:
%   x               T3DArray Struct
%                   Variable Names identical to C++ Class: T3DArray
%
%   By Karl Thiele (11/1/02)
%
% 3D DICOM for Dummies, Disclaimers and Waivers
%
% 1. Dummies refer to the R&D Staff at Philips Medical Systems.
% 2. This Matlab m-file is provided for your convenience in reading the 3D DICOM files.
% 3. The accuracy of this Matlab m-file, or the accuracy of the information contained in the
%         data files is NOT guaranteed.
% 4. No technical support will be provided.
% 5. IN NO WAY should any information derived from the 3D files be used for diagnostic purposes.
% 6. NOT FOR DIAGNOSTIC USE
% 7. The contents of this Matlab m-file has not been verified for accuracy.
% 8. For Research Only
% 9. The contents of this Matlab m-file should not be communicated to other parties
%         without the prior written consent of Philips Medical Systems
%
% Any use of this Matlab m-file implies that you agree to the
% aforementioned Disclaimers and Waivers.


% Output Disclaimer
disp('************************************');
disp('*                                  *');
```

```
disp('*  NOT FOR DIAGNOSTIC USE              *');
disp('*                                      *');
disp('****************************************');

% set default/legacy behavior
if nargin<2, MaxVolumes=0; end;

% Get Header info
fid=fopen(filename,'r','l');          % Note small L "l" for Little Endian
if(~fid) error('could not open input file'); end;

% Waste first 128 Bytes
WasteBytes  = fread(fid,128,'char');

% Waste Dicom Label
DICM   = char(fread(fid,4,'char'));

% Initialize Dicom Tags for "while" loop
TagA = 0;
TagB = 0;

% Clearly Specify the Tags used at the beginning of the data
% Note that the loop will terminate when these Tags Occur!
Data_TagA       = hex2dec('7fe0');
Data_TagB       = hex2dec('0010');

LoopCounter = 0;

while ((TagA~=Data_TagA) | (TagB~=Data_TagB)) & (LoopCounter<200)

        LoopCounter = LoopCounter + 1;

        TagA    = fread(fid,1,'ushort');
        TagB    = fread(fid,1,'ushort');
        CODE  = char(fread(fid,2,'char'))';
        N         = fread(fid,1,'ushort');

%       display([num2str(LoopCounter) ' ' num2str(TagA) ' ' num2str(TagB) ' ' CODE ' ' num2str(N)]);

        switch TagA

        case hex2dec('0018')
        if TagB==hex2dec('602c')
```

```
        DeltaX  = fread(fid,1,'double');
        elseif TagB==hex2dec('602e')
        DeltaY  = fread(fid,1,'double');
        else
        WasteBytes = fread(fid,N,'char');
        end

        case hex2dec('0028')
        if TagB==hex2dec('0008')
        tmpstr   = char(fread(fid,N,'char')');
        x.NumVolumes= sscanf(tmpstr,'%d');
        elseif TagB==hex2dec('0010')
        x.height  = fread(fid,1,'ushort');  % # of rows
        elseif TagB==hex2dec('0011')
        x.width  = fread(fid,1,'ushort');   % # of columns
        else
        WasteBytes = fread(fid,N,'char');
        end

        case hex2dec('3001')
        if TagB==hex2dec('1001')
        x.depth  = fread(fid,1,'uint');  % this is 4 bytes, vs 2 bytes
        % for rows & cols
        elseif TagB==hex2dec('1003')
        DeltaZ  = fread(fid,1,'double');
        else
        WasteBytes = fread(fid,N,'char');
        end

        otherwise
        WasteBytes  = fread(fid,N,'char');

        end

        if (CODE == 'OB') WasteBytes = fread(fid,6,'char'); end;

end


if (LoopCounter>=200)
        fclose(fid);
        error('Sorry ... somehow I became mis-aligned on the tags');
end
```

```
% Ready to Read Data: Get Volume Loop Size
N   = fread(fid,1,'uint');

% Limit the # of Volumes, and Volume Loop Size
if MaxVolumes>0,
        x.NumVolumes = MaxVolumes;
        N = x.width*x.height*x.depth*x.NumVolumes;
end;

% Finally read volume data:
x.data  = fread(fid,N,'*uint8');

% Close file
fclose(fid);

% Now Calculate the T3DArray Header Information
x.filetype          = 'Hello';
x.N                         = N;
x.N_padded      = x.N;
x.width_padded    = x.width;
x.height_padded    = x.height;
x.depth_padded    = x.depth;
x.m_Voxelsize     = 1;

x.widthspan       = x.width * DeltaX;
x.heightspan    = x.height * DeltaY;
x.depthspan       = x.depth * DeltaZ;

x.widthstart    = -x.widthspan/2;
x.heightstart    = -x.heightspan/2;
x.depthstart    = -x.depthspan/2;

x.pdata                     = 1;  % indicates that data exists

% Now we need to reshape the matrix
x.data=reshape(x.data,x.width_padded,x.height_padded,x.depth_padded,x.NumVolumes);
data = x.data;
return
```

# Appendix B

### Image Processing Code for Edge Detection: EdgeDetectHeart.m

```
clear all;
clc;
format short e
% 3Dheart at time 12 = cube (:,:,: 112);

[x,data]=readDicom3D('002A Normal lo res.dcm');
cube = data(:,:,:,12);
cube56 = cube(:,:,:,1);
%% Cube Define
dn = 9.0002;
ws = 24.8885;
Nx = dn.*ws;
Ny = dn.* 24959;
height = x.height;
heightspan = x.heightspan;
width = x.width;
widthspan = x.widthspan;
depth =  x.depth;
depthspan = x.depthspan;
sampH = 1/(heightspan./height);
sampW = 1/(widthspan./width);
sampD = 1/(depthspan./depth);
oldc = 1:1:224;
oldr = 1:1:176;
oldd = 1:1:208;
for q = 1:224
for u = 1:224
for e = 1:224
c(q,u,e) = ((width-1)./(Nx-1)).*(q-1)+1;
r(q,u,e) = ((height-1)./(Nx-1)).*(u-1)+1;
d(q,u,e) = ((depth-1)./(Nx-1)).*(e-1)+1;
end
end
end
%% Cube Scaling
 left = floor(c);
 right = left+1;
 alpha = c-left;
```

```
 up = floor(r);
 down = up+1;
 beta = r-up;
 front = floor(d);
 back = front+1;
 gamma = d-front;
counte = 0;
countu = 0;
countq = 0;
for q = 1:223
for u = 1:223
for e = 1:223
LeftUpFront =
(1-alpha(q,u,e))*(1-beta(q,u,e))*(1-gamma(q,u,e))*cube56(left(q,u,e),up(q,u,e),front(q,u,e));
RightUpFront =
(alpha(q,u,e))*(1-beta(q,u,e))*(1-gamma(q,u,e))*cube56(right(q,u,e),up(q,u,e),front(q,u,e));
LeftUpBack= (1-alpha(q,u,e))*(1-beta(q,u,e))*(gamma(q,u,e))*cube56(left(q,u,e),up(q,u,e),back(q,u,e));
RightUpBack = (alpha(q,u,e))*(1-beta(q,u,e))*(gamma(q,u,e))*cube56(right(q,u,e),up(q,u,e),back(q,u,e));
LeftDownFront =
(1-alpha(q,u,e))*(beta(q,u,e))*(1-gamma(q,u,e))*cube56(left(q,u,e),down(q,u,e),front(q,u,e));
RightDownFront =
(alpha(q,u,e))*(beta(q,u,e))*(1-gamma(q,u,e))*cube56(right(q,u,e),down(q,u,e),front(q,u,e));
LeftDownBack =
(1-alpha(q,u,e))*(beta(q,u,e))*(gamma(q,u,e))*cube56(left(q,u,e),down(q,u,e),back(q,u,e));
RightDownBack =
(alpha(q,u,e))*(beta(q,u,e))*(gamma(q,u,e))*cube56(right(q,u,e),down(q,u,e),back(q,u,e));
NewImg (q,u,e) =
LeftUpFront+RightUpFront+LeftUpBack+RightUpBack+LeftDownFront+RightDownFront+LeftDownB
ack+RightDownBack;
counte= counte+1;
end
counte = 0;
countu = countu +1;
end
countu = 0;
countq = countq +1;
end


%% Image Processing
% otsu's method
%YZ middle slice
Heart2YZ = squeeze(NewImg(112,:,:));
```

```
imwrite(Heart2YZ, 'LV2YZ.jpg');
I2YZ = imresize(Heart2YZ(:,1:min(size(Heart2YZ(:,:,1))),1), [260 260]);
Inew2YZ = imadjust(I2YZ, [0.15 0.9], []);
level2YZ = graythresh(Inew2YZ);
BW2YZ = imbinarize(Inew2YZ, level2YZ);
figure(1); clf
imshowpair(I2YZ, Inew2YZ, 'montage');
title('OG YZ and Resized YZ for Processing')
figure(2); clf
imshowpair(I2YZ, BW2YZ, 'montage');
title('OG YZ and Binarized YZ')

figure(3); clf

Inew2YZcanny = imadjust(I2YZ, [0.3 0.9], []);
BWedge2YZ = edge(Inew2YZcanny, 'Canny');
imshowpair(I2YZ, BWedge2YZ, 'montage');
title('OG YZ and Edge Detected YZ')


% trying to trace regional boundary
imwrite(Inew2YZ, 'LV2YZblackandwhite.jpg')
figure(4); clf
Itrace2YZ = imread('LV2YZblackandwhite.jpg');
BWtrace2YZ = imbinarize(Itrace2YZ);
[B2YZ, L2YZ] = bwboundaries(BWtrace2YZ, 'noholes');
imshowpair(I2YZ, (label2rgb(L2YZ, @jet, [.5 .5 .5])), 'montage')
hold on
for k2YZ = 1:length(B2YZ)
        boundary2YZ = B2YZ{k2YZ};
        plot(boundary2YZ(:,2), boundary2YZ(:, 1), 'w', 'LineWidth', 2)
end
title('OG YZ and Boundary Traced YZ')


% doing the XY plane
Heart2XY = squeeze(NewImg(:,:,112));
imwrite(Heart2XY, 'LV2XY.jpg');
I2XY = imresize(Heart2XY(:,1:min(size(Heart2XY(:,:,1))),1), [260 260]);
Inew2XY = imadjust(I2XY, [0.3 0.9], []);
level2XY = graythresh(Inew2XY);
BW2XY = imbinarize(Inew2XY, level2XY);
figure(5); clf
```

```
imshowpair(I2XY, Inew2XY, 'montage');
title('OG XY and Resized XY for Processing')
figure(6); clf
imshowpair(I2XY, BW2XY, 'montage');
title('OG XY and Binarized XY');
figure(7); clf
Inew2XYcanny = imadjust(I2XY, [0.4 0.9], []);
BWedge2XY = edge(Inew2XYcanny, 'Canny');
imshowpair(I2XY, BWedge2XY, 'montage');
title('OG XY and Edge Detected XY')
imwrite(Inew2XY, 'LV2XYblackandwhite.jpg')
figure(8); clf
Itrace2XY = imread('LV2XYblackandwhite.jpg');
BWtrace2XY = imbinarize(Itrace2XY);
[B2XY, L2XY] = bwboundaries(BWtrace2XY, 'noholes');
imshowpair(I2XY, label2rgb(L2XY, @jet, [.5 .5 .5]), 'montage')
hold on
for k2XY = 1:length(B2XY)
        boundary2XY = B2XY{k2XY};
        plot(boundary2XY(:,2), boundary2XY(:, 1), 'w', 'LineWidth', 2)
end
title('OG XY and Boundary Traced XY')
%doing the XZ plane

Heart2XZ = squeeze(NewImg(:,112,:));
imwrite(Heart2XZ, 'LV2XZ.jpg');
I2XZ = imresize(Heart2XZ(:,1:min(size(Heart2XZ(:,:,1))),1), [260 260]);
Inew2XZ = imadjust(I2XZ, [0.2 0.8], []);
level2XZ = graythresh(Inew2XZ);
BW2XZ = imbinarize(Inew2XZ, level2XZ);
figure(9); clf
imshowpair(I2XZ, Inew2XZ, 'montage')
title('OG XZ and Resized XZ for Processing')
figure(10); clf
imshowpair(I2XZ, BW2XZ, 'montage');
title('OG XZ and Binarized XZ')
figure(11); clf
Inew2XZcanny = imadjust(I2XZ, [0.3 0.8], []);
BWedge2XZ = edge(Inew2XZcanny, 'Canny');
imshowpair(I2XZ, BWedge2XZ, 'montage');
title('OG XZ and Edge Detected XZ')

imwrite(Inew2XZ, 'LV2XZblackandwhite.jpg')
```

```
figure(12); clf
Itrace2XZ = imread('LV2XZblackandwhite.jpg');
BWtrace2XZ = imbinarize(Itrace2XZ);
[B2XZ, L2XZ] = bwboundaries(BWtrace2XZ, 'noholes');
imshowpair(I2XZ, label2rgb(L2XZ, @jet, [.5 .5 .5]), 'montage')
hold on
for k2XZ = 1:length(B2XZ)
        boundary2XZ = B2XZ{k2XZ};
        plot(boundary2XZ(:,2), boundary2XZ(:, 1), 'w', 'LineWidth', 2)
end
title('OG XZ and Boundary Traced XZ')
```

# Appendix C

### Automated Slicing of the middle planes in three dimensions: AutomatedSlicing.m

```
clear all; format short e

prompt = {'The file name','Time point','Repeat measurements for how many times: '};
dlgtitle = 'Input';
dims = [2 50];
definput = {'xxx.dcm','1','3'};
answer = inputdlg(prompt,dlgtitle,dims,definput)
filename = answer{1}
timepoint = str2num(answer{2})
iteration = str2num(answer{3})

[x,data]=readDicom3D_j(filename);

cube = data(:,:,:,timepoint);
%PlotOldCube(cube)
cube56 = cube(:,:,:,1);

%% Cube Define
height = x.height;
hs = x.heightspan;
width = x.width;
ws = x.widthspan;
depth =  x.depth;
ds = x.depthspan;
sampH = 1./(hs./height);
sampW = 1./(ws./width);
sampD = 1./(ds./depth);
dW = 0.1036; % patient 1
dH = 0.169; % patient 1
dD = 0.0972319; % patient 1
% dW = 0.0786; % patient 2
% dH = 1/sampH; % patient 2
% dD = 1/sampD; % patient 2

for q = 1:depth
for u = 1:depth
for e = 1:depth
c(q,u,e) = ((q-1)./(width-1)).*(ws/dW)+1;
```

```
r(q,u,e) = ((u-1)./(height-1)).*(hs/dH)+1;
d(q,u,e) = ((e-1)./(depth-1)).*(ds/dD)+1;
end
end
end
%% Cube Scaling
 left = floor(c);
 right = left+1;
 alpha = c-left;
 up = floor(r);
 down = up+1;
 beta = r-up;
 front = floor(d);
 back = front+1;
 gamma = d-front;
counte = 0;
countu = 0;
countq = 0;
tw3=depth;
for q = 1:tw3
for u = 1:tw3
for e = 1:tw3
LeftUpFront =
(1-alpha(q,u,e))*(1-beta(q,u,e))*(1-gamma(q,u,e))*cube56(left(q,u,e),up(q,u,e),front(q,u,e));
RightUpFront =
(alpha(q,u,e))*(1-beta(q,u,e))*(1-gamma(q,u,e))*cube56(right(q,u,e),up(q,u,e),front(q,u,e));
LeftUpBack= (1-alpha(q,u,e))*(1-beta(q,u,e))*(gamma(q,u,e))*cube56(left(q,u,e),up(q,u,e),back(q,u,e));
RightUpBack = (alpha(q,u,e))*(1-beta(q,u,e))*(gamma(q,u,e))*cube56(right(q,u,e),up(q,u,e),back(q,u,e));
LeftDownFront =
(1-alpha(q,u,e))*(beta(q,u,e))*(1-gamma(q,u,e))*cube56(left(q,u,e),down(q,u,e),front(q,u,e));
RightDownFront =
(alpha(q,u,e))*(beta(q,u,e))*(1-gamma(q,u,e))*cube56(right(q,u,e),down(q,u,e),front(q,u,e));
LeftDownBack =
(1-alpha(q,u,e))*(beta(q,u,e))*(gamma(q,u,e))*cube56(left(q,u,e),down(q,u,e),back(q,u,e));
RightDownBack =
(alpha(q,u,e))*(beta(q,u,e))*(gamma(q,u,e))*cube56(right(q,u,e),down(q,u,e),back(q,u,e));
NewImg (q,u,e) =
LeftUpFront+RightUpFront+LeftUpBack+RightUpBack+LeftDownFront+RightDownFront+LeftDownB
ack+RightDownBack;
counte= counte+1;
end
counte = 0;
countu = countu +1;
```

```
end
countu = 0;
countq = countq +1;
end

%% filtering
% XY 112

cube1 = NewImg(:,:,112);
Heart1XY = squeeze(cube1);
I2XY = imresize(Heart1XY(:,1:min(size(Heart1XY(:,:,1))),1), [260 260]);
Inew1XY = imadjust(I2XY, [0.2 0.8], []);
level1XY = graythresh(Inew1XY);
BW1XY = imbinarize(Inew1XY, level1XY);

% XZ 112

cube2 = NewImg(:,112,:);
Heart1XZ = squeeze(cube2);
I2XZ = imresize(Heart1XZ(:,1:min(size(Heart1XZ(:,:,1))),1), [260 260]);
Inew1XZ = imadjust(I2XZ, [0.2 0.8], []);
level1XZ = graythresh(Inew1XZ);
BW1XZ = imbinarize(Inew1XZ, level1XZ);

% YZ 112

cube3 = NewImg(112,:,:);
Heart1YZ = squeeze(cube3);
I1YZ = imresize(Heart1YZ(:,1:min(size(Heart1YZ(:,:,1))),1), [260 260]);
Inew1YZ = imadjust(I1YZ, [0.15 0.9], []);
level1YZ = graythresh(Inew1YZ);
BW1YZ = imbinarize(Inew1YZ, level1YZ);

%% figure & select points
clear x1 y1 x2 y2 x3 y3 X1Y1 X2Y2 X3Y3 A1 A2 A3

figure(1);clf
ax1 = subplot(1,3,1)
imshow(Inew1XY)
ax2 = subplot(1,3,2)
imshow(Inew1XZ)
ax3 = subplot(1,3,3)
imshow(Inew1YZ)
```

```
for i=1:iteration
   clear x1 y1
   [x1,y1] = getpts(ax1);
   A(i) = fit_ellipse(x1,y1);
end

for i=1:iteration
   clear x2 y2
   [x2,y2] = getpts(ax2);
   B(i) = fit_ellipse(x2,y2);
end

for i=1:iteration
   clear x3 y3
   [x3,y3] = getpts(ax3);
   C(i) = fit_ellipse(x3,y3);
end

%% Calculation
x_avg = (sum([A.long_axis])+ sum([B.short_axis])) / (iteration*2)
y_avg = (sum([A.short_axis])+ sum([C.short_axis])) / (iteration*2)
z_avg = (sum([B.long_axis])+ sum([C.long_axis])) / (iteration*2)


ratio_y = y_avg/x_avg
ratio_z = z_avg/x_avg
str = sprintf('1 : %.2f : %.2f', ratio_y, ratio_z);
f = msgbox({'The ratio of x:y:z is';str},'info','help');
```